ASTRONOMY & ASTROPHYSICS
SUPPLEMENT SERIES

MARCH **1997**, PAGE 489

Astron. Astrophys. Suppl. Ser. **121,** 489-497 (1997)

Physical studies of asteroids

XXXI. Asteroid photometric observations with the Carlsberg Automatic Meridian Circle

J. Piironen[12], **P. Magnusson**[1], **C.-I. Lagerkvist**[15], **I.P. Williams**[3], **M.E. Buontempo**[4], **and L.V. Morrison**[4]

[1] Astronomiska observatoriet, Box 515, S–75120 Uppsala, Sweden
[2] Astronomical Observatory, Box 14, FIN–00014 Helsinki, Finland
[3] Queen Mary & Westfield College, Mile End Road, London E1 4NS, UK
[4] Royal Greenwich Observatory, Madingley Rd, Cambridge, CB3 0EZ, UK
[5] Institute for Planetary Exploration, DLR, Berlin, Germany

Received May 1; accepted June 10, 1996

Abstract. Photometric observations of 74 asteroids obtained with the Carlsberg Automatic Meridian Circle between January 1990 and December 1993 are presented. The data from individual asteroid apparitions have been fitted by phase curves based on the standard HG magnitude system. Statistics on mean G-values for different types of asteroids are presented. A few new determinations of asteroid rotation periods are presented. In addition, we analyse magnitude-aspect relations, and derive ellipsoidal shape models for some asteroids.

Key words: minor planets — photometry

1. Introduction

Brightness measurements at different solar phase angles have for long been one of the main sources of information constraining models of the surface micro-structure of Solar System bodies without atmospheres (Bowell et al. 1989; Hapke 1993). Despite the overwelmingly richer information content in the close-up disk-resolved space-probe images of Gaspra and Ida (Helfenstein et al. 1994 and 1996), broad phase curve surveys of many asteroids is still important in order to generalize to larger populations of minor bodies.

Previous surveys similar to this one have been published by Tedesco (1989), Lagerkvist & Magnusson (1990), and Lagerkvist et al. (1992). The last of these will be referred to as Paper I, and the current paper can be regarded as a follow-up to it, with presentation of more recent observations.

The physical interpretation of phase curves of asteroids typically are semi-empirical (Bowell et al. 1989; Hapke 1993). Theories usually predict the effect of roughness, porosity and scattering inside the surface material. The number of physical parameters involved is often quite large and there is no way that a single phase curve can give unambigous values for all. When the albedo of the asteroid is low and the scattering is geometric the theoretical interpretation gives good approximations.

2. Observations

This paper is based on observations obtained with the Carlsberg Automatic Meridian Circle (CAMC), situated at Observatorio del Roque de los Muchachos, La Palma, Spain, and operated jointly by the Copenhagen University Observatory, the Royal Greenwich Observatory, and Real Instituto y Observatorio de la Armada en San Fernando. The original observations were published in tabular form in the *Carlsberg Meridian Catalogue*, No. 6–8.

The instrument is, of course, primarily intended for astrometry, but photometric results of variable quality are obtained as a by-product. After removal of data obtained during non-photometric conditions, the remaining data have a typical accuracy of 0.05 magnitudes for 12th magnitude point sources. This modest accuracy is due to short integration times and a small aperture. However, this is compensated for by a very good solar phase angle coverage and homogeneity from apparition to apparition.

Since the instrument is constrained to the meridian, observations of a given object repeat essentially every night at the same sidereal hour. For asteroids with significant rotational light variation and a synodic spin period nearly commensurate with a day, problems may arise.

Send offprint requests to: J. Piironen

The majority of the 74 minor planets in Carlsberg Meridian Catalogues Nos. 6–8 were selected for observation for the purpose of improving their orbits in association with the Hipparcos mission. These were scheduled every second night. Some of the minor planets analysed in this paper were observed with the primary purpose of obtaining photometry for physical studies, and these were scheduled every night from western quadrature, through opposition, to eastern quadrature.

3. Basic analysis

The published V-magnitudes (Carlsberg Meridian Catalogue, Nos. 6–8) were corrected to unit heliocentric and geocentric distances to obtain the *reduced* magnitude $H(\alpha)$:

$$H(\alpha) = V - 5\log(r\Delta), \tag{1}$$

where r and Δ are the distances of the asteroid from the Sun and the Earth, respectively, and α is the solar phase angle.

In the standard HG magnitude system, as adopted at the IAU General Assembly in 1985 (Bowell et al. 1989), the reduced magnitude is modeled by the relation:

$$H(\alpha) = H - 2.5\log((1-G)\Phi_1(\alpha) + G\Phi_2(\alpha)), \tag{2}$$

which has two free parameters, the *absolute* magnitude H and the slope parameter G. The phase functions Φ_1 and Φ_2 are defined in Bowell et al. (1989). The formulation is based on a semi-empirical-semi-theoretical analysis. No physical interpretation of the slope parameter G is tied to the HG-system, although it is clear that it is related to the albedo and the proportion of multiple-scattered light.

In practice, the parameters H and G are not constants for an asteroid, but depend on the aspect angle, the obliquity angle, and the rotational phase. We take the first dependence into account by fitting Eq. (1) to the data from each apparition of the asteroid individually. This works quite well since the aspect angle is almost constant during an apparition for main-belt asteroids. Thus we get an HG-pair for each asteroid and apparition. This is in contrast to Paper I in which the G-value was constrained to be a constant for each asteroid, independent of apparition.

We will ignore the obliquity-dependence since it is probably insignificant for the moderate solar phase angles for observations of main-belt asteroids.

The dependence on rotational phase is usually removed by averaging the magnitude over a rotation cycle in the observed lightcurve. Unfortunately, the nightly sampling rate of CAMC complicates this. For objects with a high lightcurve amplitude and a rotation cycle not comensurate with a day we have added a 2nd order Fourier series to HGsystem in order to take this into account. For practical reasons we iteratively fitted the solar phase dependence and the rotational phase dependence until it converged, instead of a single least-squares fit.

4. Lightcurves

As a by-product of the phase curve fitting described above we obtain the residual rotational variation. The resulting lightcurves, obtained by folding the data with the assumed or determined rotation period, show a clear signal only if the amplitude is quite high. Note that this method will not work well if changes of the synodic period causes phase shifts during the apparition that are a significant fraction of a rotation cycle. In addition, the problem associated with the strange sampling of the present data must be stressed.

We obtain the best lightcurves for the long-period asteroids (34) Circe and (97) Klotho (see Fig. 1). We also tried to calculate a period for (570) Kyhthera from the Carlsberg data, but we obtained no unique results.

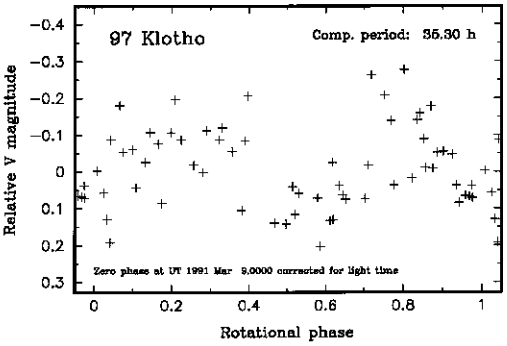

Fig. 1. Example lightcurve of 97 Klotho with data from the 1992 apparition. The magnitudes are measured relative to the fitted HG phase curve

Table 1. Estimated rotation periods

Object		Period (hours)
16	Psyche	4.196
22	Kalliope	4.148
34	Circe	16.2
97	Klotho	35.3
410	Chloris	32.53
423	Diotima	4.30

The period estimations of the lightcurve give fitting errors of only a few percent. This may be misleading in cases where aspect changes cause the synodic period to vary. However, the known periods for (16) Psyche, (22) Kalliope, (410) Chloris and (423) Diotima produced the best lightcurves after Fourier- fitting to the known periods. If the other periods from the Fourier-fit were chosen it was not possible to produce any kind of lightcurve. Most of the

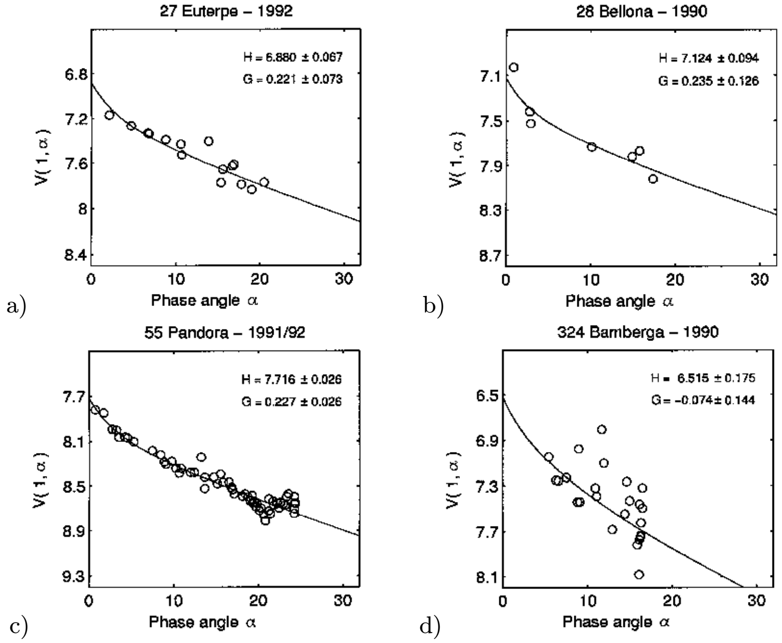

Fig. 2. Four example phase curves illustrating a variation of sampling frequency and scatter in the magnitude measurements. Note that 27 Euterpe seems to have a linear phase curve and 28 Bellona may have a steep opposition spike. However, the data is not really good enough for that kind of detailed analysis

periods from the Fourier-fitting are thus artifacts of the sparse data points, and thus the only reliable indicator of the goodness of fitting is the goodness of the produced lightcurve. The estimated rotation periods are presented in Table 1.

5. Phase curves

The analysis gave over two hundred phase curves for 74 asteroids. We have studied them all graphically. In Fig. 2 we show four representative examples. The results are summarized numerically in Table 5.

A major problem with phase curve fitting is that for objects that do not follow closely the HG-law the determined H and G-value will depend on the solar phase angle range used.

The phase curves are quite linear in 15 cases out of 74 asteroids included in this study (see Fig. 2a for an example). For these the HG-fit is misleading and may predict non-existent physical properties. The linearity of the phase curve is most evident for (5) Astraea, (9) Metis, (12) Victoria, (27) Euterpe, (51) Nemausa, (88) Thisbe, (129) Antigone and (511) Davida. The linearity does not seem to depend much on taxonomic type.

Indications of opposition spikes, which could be caused by coherent backscatter of surface material (Muinonen 1990; Skhuratov & Muinonen 1991), is evident for (28) Bellona, (37) Fides, (44) Nysa, (77) Frigga, (97) Klotho, (196) Philomela and och (349) Dembowska (see Fig. 2b for an example).

Table 2 shows average slope parameters G for different taxonomic categories. Our data is in good agreement with previous results (Harris & Young 1988; Lagerkvist & Magnusson 1990; Lagerkvist et al. 1992). Although the dispersion of G-values for individual taxonomic types is quite big the G-values is a useful indicator of the approximate albedo.

6. Aspect dependence

In addition to the HG-analysis presented here we have made exactly the same analysis for the 1984 to 1989 Carlsberg data. Combining the two data sets we get a 10-year coverage for some asteroids. This gives quite good statistics on how the phase curves change with opposition longitude. For asteroids with a known spin vector direction we can further compute the aspect angle of the observations. In this paper we define the aspect angle θ as the angle between the asteroid spin vector and the reverse of the phase angle bisector (PAB). Spin vectors were taken from the collection of spin vector determinations by Magnusson et al. (1994). We used the first synthesis solution for each asteroid. Aspect angles for 23 of our current sample of asteroids were obtained in this way. We have looked at graphs of the dependence of H and G on the aspect angle θ for all these objects. Examples of the H-dependence are shown in Fig. 3.

Table 2. Mean slope parameters G for different taxonomic groups ordered according to there albedo. For each group and reference, N is the number of asteroids included, $< G >$ is the average G-value and "Disp" is the corresponding dispersion

Taxonomy	Harris and Young (1988)			Lagerkvist and Magnusson (1990)			Paper I			This paper		
	N	$< G >$	Disp	N	$< G >$	Disp	N	$< G >$	Disp	N	$< G >$	Disp
(low albedo)												
CGBFPTD	37	0.09	0.09	28	0.09	0.07	11	0.12	0.07	26	0.10	0.06
M	11	0.21	0.06	11	0.22	0.05	5	0.19	0.06	8	0.19	0.07
SQ	31	0.23	0.11	26	0.23	0.11	28	0.23	0.05	34	0.25	0.10
EVR	4	0.42	0.08	4	0.41	0.06	3	0.37	0.04	3	0.35	0.04
(high albedo)												

For objective analysis of these graphs we fit 2nd order Legendre series:

$$\begin{aligned} G &= \sum_{n=0}^{2} g_n P_n(\cos\theta) = g_0 + g_1 \cos\theta \\ &+ \frac{g_2}{4}(3\cos 2\theta + 1) \end{aligned} \tag{3}$$

$$\begin{aligned} H(\alpha_0) &= \sum_{n=0}^{2} h_n P_n(\cos\theta) = h_0 + h_1 \cos\theta \\ &+ \frac{h_2}{4}(3\cos 2\theta + 1). \end{aligned}$$

Light scattering is probably closest to the geometric approximation at zero solar phase. Therefore the modeled reduced magnitude H at $\alpha_0 = 0°$ is usually used. However, in practice this value is obtained from extrapolation from observed solar phases, and thus sensitive to errors in the slope parameter G. In order to reduce this source of error we instead use the model magnitude at $\alpha_0 = 13°$, which is near the mean observed solar phase angle.

For most asteroids there are two symmetric spin vector solutions that both fit the observations equally well. If the second synthesis solution in Magnusson (1996) is choosen instead of the first one then approximately the same coefficients results, except that h_1 and g_1 have opposite sign.

6.1. *H-dependence*

The Legendre coefficients for 23 asteroids are presented in Table 3. The tabulated error estimates are based on the quality of fit. The variations in $H(13°)$ are probably due to changing geometrical cross-sections, and, to lesser extent, differences in average albedo at different latitudes on the asteroid surfaces. Non-zero coefficients h_1 are most naturally interpreted as differences in albedo on the northern and southern hemispheres. The second Legendre component is probably due mostly to polar flattening, as evident from the clear dominance of negative h_2-values in Table 3. However, differences in albedo between equatorial and polar regions may also contribute to h_2.

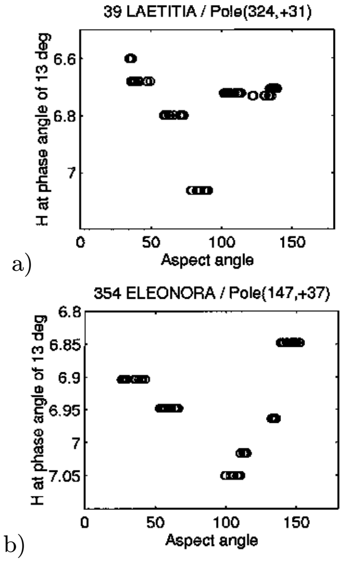

Fig. 3. Two good examples of the aspect dependence of the slope parameter H. Both show a "U-shaped" pattern typical of bodies with polar flattening. The values above the diagrams are ecliptic coordinates of the spin vector used

The Legendre coefficients are a natural way of descibing the light scattering, but most asteroid shape models take the form of tri-axial ellipsoids with axis-ratios $a \geq b \geq c$ (Magnusson et al. 1989). These models are often based on extensive lightcurve photometry, with lightcurve amplitudes giving quite reliable ratios a/b. However, the b/c-ratios are often ill-defined because amplitudes give very model-dependent b/c-values and the absolute calibration of lightcurve photometry are often heterogenous. The Carlberg data have the opposite characteristics, i.e. homogenous absolute calibration and bad lightcurves, and they therefore complement standard photometry well. We therefore use a/b-ratios from other models as input, and compute b/c-ratios from the Carlsberg data.

The difference between the mean polar H-value and the equatorial H-value is $H_{\rm pol} - H_{\rm eq} = \frac{3}{2}h_2$. By equating the corresponding brightness ratio, $10^{-\frac{2}{5}(H_{\rm pol}-H_{\rm eq})}$, with

Table 3. A summary of the Legendre coefficients

Asteroid	h_0	h_1	h_2
3	5.93 ± 0.05	$+0.03 \pm 0.08$	-0.26 ± 0.19
4	3.74 ± 0.04	-0.09 ± 0.06	-0.31 ± 0.14
5	7.61 ± 0.05	$+0.15 \pm 0.10$	-0.37 ± 0.36
7	6.37 ± 0.03	$+0.12 \pm 0.06$	-0.24 ± 0.08
9	7.10 ± 0.07	-0.12 ± 0.14	-0.57 ± 0.14
10	6.21 ± 0.03	-0.01 ± 0.04	-0.01 ± 0.07
15	5.91 ± 0.07	-0.03 ± 0.07	-0.19 ± 0.16
16	6.70 ± 0.04	-0.04 ± 0.08	-0.37 ± 0.09
17	8.36 ± 0.02	$+0.15 \pm 0.04$	-0.31 ± 0.06
19	7.98 ± 0.02	$+0.06 \pm 0.03$	$+0.21 \pm 0.13$
22	7.27 ± 0.07	$+0.08 \pm 0.12$	-0.23 ± 0.24
29	6.58 ± 0.03	-0.02 ± 0.07	-0.10 ± 0.08
39	6.72 ± 0.03	$+0.01 \pm 0.06$	-0.18 ± 0.09
44	7.53 ± 0.07	-0.16 ± 0.11	-0.06 ± 0.25
45	8.21 ± 0.04	$+0.04 \pm 0.07$	-0.13 ± 0.11
51	8.02 ± 0.14	-0.09 ± 0.12	-0.57 ± 0.36
55	8.52 ± 0.02	$+0.09 \pm 0.03$	-0.41 ± 0.04
63	8.02 ± 3.00	$+0.31 \pm 5.41$	-0.80 ± 3.30
129	7.57 ± 0.07	$+0.22 \pm 0.12$	-0.53 ± 0.20
216	6.40 ± 0.38	-2.63 ± 0.70	-1.85 ± 0.37
349	6.51 ± 0.02	-0.10 ± 0.03	-0.03 ± 0.03
354	6.97 ± 0.01	$+0.01 \pm 0.02$	-0.16 ± 0.03
511	6.89 ± 0.05	-0.11 ± 0.06	$+0.23 \pm 0.09$

Table 4. Ellipsoidal model axis ratios

Asteroid	From the literature		Computed
	a/b	b/c	b/c
7	1.23 ± 0.05	1.30 ± 0.10	1.26 ± 0.15
10	1.29 ± 0.05	0.90 ± 0.30	0.90 ± 0.09
16	1.30 ± 0.10	1.30 ± 0.10	1.48 ± 0.19
17	1.25 ± 0.10	1.40 ± 0.10	1.32 ± 0.12
19	1.24 ± 0.10	1.00 ± 0.10	0.66 ± 0.12
29	1.10 ± 0.10	1.10 ± 0.05	1.10 ± 0.13
39	1.47 ± 0.05	1.40 ± 0.20	1.07 ± 0.14
45	1.36 ± 0.05	1.40 ± 0.20	1.04 ± 0.15
55	1.29 ± 0.05	1.30 ± 0.10	1.57 ± 0.10
349	1.31 ± 0.05	1.12 ± 0.05	0.92 ± 0.04
354	1.21 ± 0.05	1.10 ± 0.10	1.14 ± 0.05
511	1.24 ± 0.05	1.12 ± 0.05	0.66 ± 0.08

the ratio between the area of the projection of the model along the spin axis, (πab), and the mean perpendicular cross-section, $\pi c(a+b)/2$, and solving for b/c, we obtain the approximate relation:

$$\frac{b}{c} \approx \frac{1}{2}\left(1+\frac{b}{a}\right) 10^{-\frac{3}{5}h_2}. \tag{4}$$

Table 4 shows the axes ratios for the best cases where the errors are not too high. The accuracy seems to be similar to the dispersion of b/c-values from ordinary photometry (Magnusson, in preparation). The number of apparitions is so low that a single bad phase curve can easily ruin the Legendre fit.

6.2. G-dependence

For most of the objects no significant variation of G-values were found to indicate any clear aspect dependence. In general the estimated errors in g_1 and g_2 are of the same order as the values themselves. We find, however, some indication of different G-values between the northern and southern hemispheres for the cases of (7) Iris and (16) Psyche, but this has to be confirmed by further observations. The latter case may confirm the finding by Lupishko & Belskaya (1983) and Lupishko et al. (1983) that (16) Psyche is among the objects that have different albedos on the hemispheres.

In general the variations in G are probably associated with surface variegation, different compositional and morphological surface areas, and global shape effects. However, we are perplexed by the clear dominance of negative g_2-values, which is opposite to our expectations. To see why, let us consider equatorial lightcurves. These generally show a clear increase in lightcurve amplitude as the solar phase angle increases. Within the framework of triaxial models, with semi-axes $a \geq b \geq c$, this implies that the G-value measured along the a-axis (looking down at the point of highest curvature) is smaller than the G-value measured along the b-axis. We expected a continuation of this trend with even larger G-values when observing along the c-axis, which show the flat polar regions with the lowest curvature in the model. The result would have been positive g_2-values.

7. Discussion

The Carlbserg Meridian Circle photometry is quite useful for doing coarse phase curve studies of asteroids. A weakness is that an object is measured only once per night. Good knowledge about the rotational light variation is required in order to subtract this variation and obtain good phase curves. A good property is the excellent range of solar phase angles, often covering a large part of the interval from 0° to 30°, which is more than one usually finds for manual photometric observations.

Phase curves measured in the period 1990 to 1993 indicate that one should be careful in determining the physical properities of an asteroids if the range of phase angles is not high enough. The H and G-values are very sensitive to range and amount of data.

Finally axial ratio estimation of asteroid shapes is a new way to make Carslberg Meridian Circle data useful. The b/c-values obtained here have probable errors of about the same size as the dispersion in the values obtained from inversion of lightcurves. The shape determination would benefit from a few additional apparitions of data. Also, as more spin axis determinations become available a larger fraction of the CAMC observations will become useful for shape determination.

Acknowledgements. Jukka Piironen was supported by the NorFA-foundation (Oslo, Norway). Per Magnusson was supported by the Swedish National Space Board ("Rymdstyrelsen") and by the Swedish Natural Science Research Council ("NFR").

References

Bowell E., Hapke B., Domingue D., Lumme K., Peltoniemi J., Harris A.W., 1989, Application of Photometric Models to Asteroids. In Asteroids II, Binzel R.P., Gehrels T., Matthews M.S. (eds.). Univ. Arizona Press., pp. 524–556

Carlsberg Meridian Catalogue, La Palma, No. 6–8, 1992–1994, Copenhagen University Observatory, Royal Greenwich Observatory, and Real Instituto y Observatorio de la Armada en San Fernando

Hapke B., 1993, Theory of Reflectance and Emittance Spectroscopy. Series: Topics in Remote Sensing 3. Cambridge Univ. Press

Harris A.W., Young J.W., 1988, Observations of asteroid phase relations, BAAS 20, 865

Helfenstein P., Veverka J., Thomas P.C., et al., 1994, Galileo photometry of asteroid 951 Gaspra. Icarus 107, 37–60

Helfenstein P., Veverka J., Thomas P.C., et al., 1996, Galileo photometry of asteroid 243 Ida (submitted to Icarus)

Lagerkvist C.-I., Magnusson P., 1990, Analysis of asteroid lightcurves. II. Phase curves in a generalized HG-system, A&AS 78, 519–532

Lagerkvist C.-I., Magnusson P., Williams I.P., et al., 1992, Physical studies of asteroids XXIV: Phase relations for 48 asteroids obtained with the Carlsberg Meridian Circle, A&AS 94, 43–71

Lupishko D.F., Belskaya I.N., 1983, Surface, shape and rotation of the M-type asteroid 16 Psyche from UBV-photometry in 1978 and 1979, in Asteroids, Comets, Meteors, Uppsala University, Uppsala, Sweden, pp. 55–62

Lupishko D.F., Akimov L.A., Belskaya I.N., 1983, On photometric heterogenity of asteroid surfaces, in Asteroids, Comets, Meteors, Uppsala University, Uppsala, Sweden, pp. 63–70

Magnusson P., 1996 (in preparation)

Muinonen K., 1990, Light Scattering by Inhomogenous Media: Backward Enhancement and Reversal of Linear polarization, PhD. Dissertation, University of Helsinki, Finland

Shkuratov Yu.G., Muinonen K., 1991, Interpretating Asteroid Photometry and Polarimetry Using A Model of Shadowing and Coherent Backscatter, Asteroids, Comets, Meteors 1991, pp. 549–552

Tedesco E.F., 1989, Asteroid magnitudes, UBV colors, and IRAS albedos and diameters, in Asteroids II, Binzel R.P., Gehrels T., Matthews M.S. (eds.). Univ. Arizona Press., pp. 1090–1138

Table 5. Results of *HG*-fits to the data of each asteroid and apparition. The columns give the *H* and *G*-values with their estimated errors, the number *N* of magnitude measurements, the root-mean-square error of the fit, and the phase angle range (degrees) of the data. Note that we have included all results, even when the size of the uncertainty is comprable to the value. The mean *H* and *G*-values for each asteroid were computed with weights taking the error estimates for individual apparitions into account

Year	H	G	N	α–range
1 Ceres				
1990	3.29 ± 0.12	0.08 ± 0.09	13	10.5–21.9
1991	3.31 ± 0.03	0.07 ± 0.02	17	5.3–22.0
1992	3.39 ± 0.05	0.20 ± 0.05	18	3.8–19.5
Mean	3.33	0.09		
2 Pallas				
1991	4.07 ± 0.04	0.02 ± 0.04	13	4.6–23.6
3 Juno				
1990	5.32 ± 0.05	0.36 ± 0.06	31	4.8–17.4
1991	5.30 ± 0.06	0.35 ± 0.07	22	5.7–21.2
1992	5.06 ± 0.10	0.17 ± 0.09	9	10.9–27.6
Mean	5.28	0.31		
4 Vesta				
1992	3.19 ± 0.06	0.32 ± 0.06	10	4.9–25.3
5 Astraea				
1991	7.01 ± 0.11	0.35 ± 0.10	7	3.5–25.10
1992	7.04 ± 0.09	0.37 ± 0.11	17	2.7–21.0
1993	6.90 ± 0.06	0.32 ± 0.08	14	1.1–19.4
Mean	6.95	0.34		
6 Hebe				
1990	5.68 ± 0.09	0.16 ± 0.09	36	7.3–19.3
1991	5.81 ± 0.07	0.33 ± 0.07	19	3.7–29.7
1992/93	5.67 ± 0.09	0.26 ± 0.09	10	2.9–22.8
Mean	5.74	0.26		
7 Iris				
1990	5.50 ± 0.05	0.27 ± 0.07	31	1.5–19.7
1991	5.71 ± 0.10	0.43 ± 0.12	17	5.6–29.5
1992	5.36 ± 0.12	0.17 ± 0.10	6	3.8–23.2
Mean	5.52	0.28		
8 Flora				
1990	6.42 ± 0.03	0.27 ± 0.04	25	1.3–22.1
1992	6.52 ± 0.01	0.37 ± 0.02	8	1.3–25.2
1993	6.60 ± 0.05	0.36 ± 0.07	13	3.6–20.1
Mean	6.51	0.36		
9 Metis				
1991	6.45 ± 0.06	0.25 ± 0.06	10	5.6–24.1
1992	6.42 ± 0.11	0.20 ± 0.12	17	0.7–21.8
Mean	6.45	0.24		
10 Hygiea				
1990	5.40 ± 0.07	0.22 ± 0.09	27	1.6–17.4
1991/92	5.47 ± 0.05	0.15 ± 0.05	44	1.2–16.4
1992/93	5.44 ± 0.03	0.26 ± 0.03	43	0.3–16.6
Mean	5.44	0.22		
11 Parthenope				
1991	6.58 ± 0.03	0.19 ± 0.03	4	2.3–21.0
1992	6.69 ± 0.07	0.20 ± 0.08	16	3.3–22.0
Mean	6.60	0.19		
12 Victoria				
1990/91	7.41 ± 0.09	0.36 ± 0.10	6	3.6–19.6
1992	7.06 ± 0.05	0.18 ± 0.04	7	5.7–23.5
1993	7.55 ± 0.30	0.43 ± 0.33	4	7.1–25.3
Mean	7.14	0.21		
13 Egeria				
1990	6.63 ± 0.86	0.05 ± 0.76	4	12.7–16.1
1991/92	7.13 ± 0.22	0.54 ± 0.27	8	9.0–23.9
1993	6.60 ± 0.08	0.14 ± 0.08	11	1.6–22.1
Mean	6.66	0.17		
14 Irene				
1992	6.49 ± 0.51	0.26 ± 0.45	9	9.1–27.2
15 Eunomia				
1990/91	5.26 ± 0.12	0.23 ± 0.15	9	2.2–23.2
1992	5.35 ± 0.15	0.28 ± 0.19	10	5.5–16.5
Mean	5.29	0.24		
16 Psyche				
1990/91	5.93 ± 0.04	0.22 ± 0.04	31	3.6–22.4
1991/92	5.98 ± 0.04	0.20 ± 0.05	48	1.5–18.0
1993	5.68 ± 0.02	0.23 ± 0.03	50	2.5–17.3
Mean	5.78	0.22		
17 Thetis				
1990/91	7.66 ± 0.19	0.21 ± 0.19	4	5.0–18.10
1992	7.83 ± 0.21	0.43 ± 0.25	16	4.5–24.7
Mean	7.74	0.29		
18 Melpomene				
1990	6.41 ± 0.05	0.17 ± 0.06	18	1.9–20.5
1991	6.66 ± 0.12	0.33 ± 0.14	16	6.8–23.3
1992/93	6.37 ± 0.12	0.09 ± 0.09	11	6.2–20.4
Mean	6.44	0.17		
19 Fortuna				
1992	7.15 ± 0.13	0.12 ± 0.13	11	3.2–18.0
1993	7.00 ± 0.05	0.04 ± 0.04	17	1.2–26.3
Mean	7.02	0.05		
20 Massalia				
1991/92	6.47 ± 0.11	0.22 ± 0.09	13	2.7–28.5
1993	6.50 ± 0.06	0.25 ± 0.07	13	2.7–20.8
Mean	6.49	0.23		
21 Lutetia				
1991	7.47 ± 0.06	0.14 ± 0.07	36	2.0–19.4
1992	7.36 ± 0.02	0.13 ± 0.02	82	1.4–28.5
Mean	7.37	0.13		
22 Kalliope				
1990	6.48 ± 0.06	0.29 ± 0.08	40	7.1–19.6
1991/92	6.57 ± 0.06	0.20 ± 0.06	35	2.7–22.3
1990	6.32 ± 0.03	0.21 ± 0.03	54	6.4–19.2
Mean	6.39	0.22		
23 Thalia				
1990	6.93 ± 0.08	0.25 ± 0.08	22	7.3–25.8
1991	6.98 ± 0.08	0.11 ± 0.09	18	3.3–16.7
1992	6.97 ± 0.09	0.26 ± 0.09	11	5.0–20.7
Mean	6.96	0.21		

Year	H	G	N	α–range
24 Themis				
1990/91	7.13 ± 0.23	0.16 ± 0.22	6	9.3–19.3
1992	7.16 ± 0.09	0.25 ± 0.10	11	3.4–18.3
Mean	7.16	0.24		
27 Euterpe				
1990/91	7.05 ± 0.06	0.31 ± 0.07	8	1.0–30.2
1992	6.88 ± 0.07	0.22 ± 0.07	16	2.1–20.5
Mean	6.97	0.27		
28 Bellona				
1990	7.12 ± 0.09	0.23 ± 0.13	7	0.9–17.3
1991/92	7.14 ± 0.11	0.19 ± 0.12	8	5.7–17.9
Mean	7.13	0.21		
29 Amphitrite				
1990	5.81 ± 0.19	0.43 ± 0.22	11	0.9–17.3
1993	6.00 ± 0.15	0.15 ± 0.17	10	11.8–23.4
Mean	5.93	0.25		
30 Urania				
1991	7.74 ± 0.13	0.20 ± 0.13	9	1.4–21.5
1992	7.50 ± 0.05	0.29 ± 0.06	13	1.1–20.5
1993	7.53 ± 0.02	0.25 ± 0.02	4	4.0–26.0
Mean	7.53	0.25		
34 Circe				
1990/91	8.42 ± 0.06	0.07 ± 0.05	33	3.1–23.6
1992	8.54 ± 0.06	0.07 ± 0.05	59	3.1–21.2
1993	8.53 ± 0.02	0.15 ± 0.03	58	1.1–19.1
Mean	8.52	0.12		
35 Leukothea				
1990	8.25 ± 0.15	0.08 ± 0.12	16	4.6–23.6
1991	8.63 ± 0.05	0.04 ± 0.06	66	2.1–17.6
1993	8.45 ± 0.07	0.10 ± 0.08	13	3.3–15.4
Mean	8.54	0.07		
37 Fides				
1990	7.34 ± 0.05	0.27 ± 0.07	19	1.5–22.0
1991	7.39 ± 0.08	0.30 ± 0.12	14	2.1–18.9
1992	7.39 ± 0.06	0.33 ± 0.08	11	1.5–22.1
1993	7.15 ± 0.11	0.14 ± 0.09	5	12.4–26.4
Mean	7.35	0.27		
38 Leda				
1990	8.15 ± 0.07	0.09 ± 0.07	31	2.6–20.3
1991/92	8.45 ± 0.07	0.05 ± 0.05	30	1.2–24.4
1993	8.48 ± 0.09	0.22 ± 0.11	46	3.8–20.5
Mean	8.35	0.08		
39 Laetitia				
1990	6.10 ± 0.11	0.21 ± 0.12	24	3.0–18.3
1991	5.98 ± 0.05	0.19 ± 0.05	17	5.1–21.9
1992/93	6.30 ± 0.22	0.15 ± 0.20	11	6.7–22.6
Mean	6.02	0.19		
40 Harmonia				
1990	7.07 ± 0.10	0.21 ± 0.08	16	3.5–27.2
1991/92	7.19 ± 0.11	0.20 ± 0.09	10	2.4–25.6
1993	7.17 ± 0.06	0.33 ± 0.07	12	2.0–23.4
Mean	7.15	0.26		
42 Isis				
1990	7.39 ± 0.17	0.16 ± 0.13	7	8.4–28.0
1992	7.53 ± 0.14	0.28 ± 0.14	9	2.9–19.5
1993	7.79 ± 0.19	0.41 ± 0.26	9	4.8–22.0
Mean	7.55	0.24		
44 Nysa				
1990	6.94 ± 0.14	0.52 ± 0.19	9	1.3–22.4
1991/92	6.62 ± 0.17	0.20 ± 0.13	10	5.6–27.8
1993	6.97 ± 0.07	0.53 ± 0.11	13	1.8–21.4
Mean	6.93	0.41		
45 Eugenia				
1991	7.26 ± 0.06	0.06 ± 0.05	8	2.9–21.1
1992	7.26 ± 0.04	0.13 ± 0.04	14	3.6–21.0
Mean	7.26	0.11		
50 Virginia				
1990	8.99 ± 0.12	0.15 ± 0.31	9	1.8–8.1
1991/92	9.28 ± 0.13	0.17 ± 0.10	27	3.0–30.1
1993	8.71 ± 0.14	0.22 ± 0.12	30	0.9–15.0
Mean	9.00	0.16		
51 Nemausa				
1990	7.29 ± 0.10	0.11 ± 0.08	11	4.2–22.3
1991/92	7.43 ± 0.18	0.15 ± 0.15	6	8.4–24.5
1993	7.44 ± 0.08	0.10 ± 0.07	12	8.1–26.1
Mean	7.38	0.11		
52 Europa				
1990	6.06 ± 0.03	0.16 ± 0.04	23	2.9–16.0
1991	6.30 ± 0.08	0.01 ± 0.08	16	0.9–14.8
1992	6.21 ± 0.06	0.15 ± 0.07	9	3.9–17.1
Mean	6.11	0.14		
55 Pandora				
1990	7.63 ± 0.15	0.32 ± 0.22	27	3.4–17.9
1991/92	7.72 ± 0.03	0.23 ± 0.03	59	0.7–24.3
1992/93	7.92 ± 0.05	0.10 ± 0.05	44	3.6–20.3
Mean	7.76	0.20		
63 Ausonia				
1991	7.97 ± 0.79	0.58 ± 0.96	11	11.1–23.9
1992	7.78 ± 0.36	0.32 ± 0.40	11	3.2–22.6
Mean	7.81	0.36		
68 Leto				
1990	6.88 ± 0.07	0.31 ± 0.11	14	3.2–20.7
1991	7.09 ± 0.06	0.31 ± 0.08	15	0.3–18.2
1992	6.83 ± 0.08	0.16 ± 0.07	15	5.8–25.5
Mean	6.95	0.24		
74 Galatea				
1991	8.64 ± 0.04	0.08 ± 0.05	58	1.7–18.0
75 Eurydike				
1991	9.09 ± 0.11	-0.01 ± 0.14	23	1.1–15.6
1992	9.03 ± 0.10	-0.22 ± 0.08	18	0.9–16.9
1993	9.02 ± 0.04	0.13 ± 0.03	71	0.8–30.1
Mean	9.03	0.12		
77 Frigga				
1990	8.28 ± 0.31	0.03 ± 0.20	4	16.0–22.6
1991	8.76 ± 0.06	0.11 ± 0.06	41	0.5–20.4
1992	8.45 ± 0.17	0.15 ± 0.12	24	7.7–19.5
1993	8.57 ± 0.03	0.13 ± 0.03	54	1.9–23.8
Mean	8.60	0.13		
87 Sylvia				
1993	6.64 ± 0.22	0.01 ± 0.18	14	9.5–15.3
88 Thisbe				
1990	7.01 ± 0.05	0.20 ± 0.05	27	1.8–22.6
1991	6.98 ± 0.05	0.06 ± 0.05	12	3.0–22.2
1992/93	7.07 ± 0.04	0.15 ± 0.05	8	1.1–22.1
Mean	7.02	0.14		
89 Julia				
1991	6.57 ± 0.07	0.08 ± 0.06	8	6.4–17.5
97 Klotho				
1990	7.54 ± 0.09	0.17 ± 0.11	15	0.5–18.1
1991	7.87 ± 0.03	0.22 ± 0.04	61	4.9–17.0
1992	7.78 ± 0.02	0.13 ± 0.03	67	3.7–20.9
Mean	7.80	0.15		

Year	H	G	N	α–range
114 Kassandra				
1993	8.15 ± 0.05	0.05 ± 0.05	68	2.8–20.3
115 Thyra				
1991	7.94 ± 0.16	0.63 ± 0.21	14	9.6–21.4
1992	7.77 ± 0.10	0.40 ± 0.12	12	4.4–27.4
Mean	7.82	0.45		
117 Lomia				
1990	7.90 ± 0.06	0.04 ± 0.07	28	1.1–16.8
1991/92	7.76 ± 0.11	0.06 ± 0.08	28	7.5–19.3
1992/93	7.93 ± 0.06	0.05 ± 0.06	38	0.9–18.9
Mean	7.89	0.05		
119 Althaea				
1993	8.36 ± 0.07	0.17 ± 0.07	67	3.5–20.9
129 Antigone				
1990	6.91 ± 0.06	0.25 ± 0.08	29	3.3–22.8
1991	7.11 ± 0.13	0.27 ± 0.15	21	0.8–21.2
1992/93	7.02 ± 0.10	0.33 ± 0.12	11	5.2–16.6
Mean	6.96	0.27		
192 Nausikaa				
1990	7.40 ± 0.62	0.20 ± 0.47	5	19.9–25.8
1991	7.43 ± 0.04	0.36 ± 0.05	10	1.4–19.3
1992	7.36 ± 0.08	0.22 ± 0.10	10	5.8–18.9
Mean	7.42	0.34		
196 Philomela				
1990	6.35 ± 0.05	0.20 ± 0.06	25	1.6–16.1
1991	6.63 ± 0.09	0.18 ± 0.11	16	3.4–16.8
1992/93	6.38 ± 0.03	0.17 ± 0.04	10	1.2–17.0
Mean	6.39	0.18		
216 Kleopatra				
1992	7.11 ± 0.23	0.05 ± 0.27	9	3.6–14.5
1993	6.96 ± 0.12	0.45 ± 0.20	9	4.0–15.5
Mean	6.99	0.31		
230 Athamantis				
1991	7.62 ± 0.05	0.49 ± 0.07	11	5.6–21.9
1992	7.48 ± 0.05	0.43 ± 0.06	15	6.2–24.6
Mean	7.54	0.46		
233 Asterope				
1993	8.59 ± 0.21	0.06 ± 0.19	39	0.8–23.5
243 Ida				
1991/92	9.84 ± 0.31	0.06 ± 0.35	12	0.6–13.7
1993	9.80 ± 0.41	0.03 ± 0.55	16	3.4–10.9
Mean	9.83	0.05		
308 Polyxo				
1993	8.15 ± 0.05	0.17 ± 0.05	67	1.0–20.8
324 Bamberga				
1990	6.51 ± 0.17	0.07 ± 0.14	24	5.4–16.5
1991	6.89 ± 0.05	0.05 ± 0.04	19	4.7–31.1
1992/93	6.71 ± 0.20	0.09 ± 0.14	7	3.1–19.2
Mean	6.85	0.05		
337 Devosa				
1990	8.73 ± 0.15	0.37 ± 0.18	21	4.9–22.9
1991	8.83 ± 0.03	0.19 ± 0.04	55	2.3–22.9
Mean	8.83	0.20		
349 Dembowska				
1990	5.90 ± 0.08	0.29 ± 0.11	25	1.5–18.2
1991	6.00 ± 0.07	0.45 ± 0.09	16	4.8–21.4
1992/93	5.84 ± 0.12	0.13 ± 0.14	10	3.0–19.9
Mean	5.94	0.33		
354 Eleonora				
1992	6.29 ± 0.10	0.26 ± 0.10	18	10.3–20.6
1993	6.14 ± 0.04	0.09 ± 0.04	16	3.2–18.5
Mean	6.16	0.11		
410 Chloris				
1990	8.24 ± 0.09	0.14 ± 0.10	35	5.2–19.1
423 Diotima				
1990	7.04 ± 0.09	0.24 ± 0.11	25	5.1–17.6
1992	6.82 ± 0.04	0.01 ± 0.03	48	1.2–18.1
Mean	6.85	0.03		
451 Patientia				
1990	6.55 ± 0.10	0.05 ± 0.10	4	5.4–18.8
1991/92	6.42 ± 0.09	0.01 ± 0.08	8	7.0–18.8
1992/93	6.58 ± 0.15	0.16 ± 0.17	9	8.6–17.6
Mean	6.49	0.04		
471 Papagena				
1990	6.97 ± 0.20	0.45 ± 0.24	17	6.8–23.0
1991/92	7.05 ± 0.29	0.47 ± 0.31	12	10.0–23.5
1992/93	6.56 ± 0.09	0.38 ± 0.11	9	5.9–17.1
Mean	6.66	0.40		
511 Davida				
1991/92	6.31 ± 0.25	0.17 ± 0.23	9	5.0–21.7
1993	6.32 ± 0.17	0.22 ± 0.20	13	6.7–16.2
Mean	6.32	0.20		
532 Herculina				
1990/91	5.84 ± 0.04	0.30 ± 0.05	7	2.2–22.6
1992	5.78 ± 0.05	0.14 ± 0.05	21	7.1–24.4
1993	5.90 ± 0.05	0.22 ± 0.06	17	5.6–17.7
Mean	5.84	0.22		
570 Kythera				
1993	8.32 ± 0.07	0.06 ± 0.09	46	0.4–13.8
704 Interamnia				
1990	6.07 ± 0.11	0.05 ± 0.09	5	10.1–18.8
1992	6.01 ± 0.07	0.02 ± 0.05	3	10.5–17.4
1992/93	6.00 ± 0.13	0.02 ± 0.13	9	6.4–16.9
Mean	6.01	0.06		